16th World Conference on Earthquake, 16WCEE 2017

Santiago Chile, January 9th to 13th 2017

Paper N° 2207

Registration Code: S- J14663441874

NONLINEAR MODELING OF THE SEISMIC PERFORMANCE OF A BUILDING AT SANKHU DURING THE 2015 NEPAL EARTHQUAKE

S. Bose[1], A. Nozari[2], A. Stavridis[3], B. Moaveni[4]

[1] PhD Student, Dept. of Civil Structural and Environmental Engineering, University at Buffalo, supratik@buffalo.edu

[2] PhD Student, Dept. of Civil and Environmental Engineering, Tufts University, amin.nozari@tufts.edu

[3] Assistant Professor, Dept. of Civil Structural and Environmental Engineering, University at Buffalo, astavrid@buffalo.edu

[4] Associate Professor, Dept. of Civil and Environmental Engineering, Tufts University, babak.moaveni@tufts.edu

Abstract

This paper discusses the simulation of the structural performance of a four-story school building in Sankhu, Nepal after the 2015 Gorkha Earthquake. The structure had a masonry-infilled reinforced concrete frame, which was severely damaged during the earthquake. The concentration of damage in the south end of the ground story indicates that the frame exhibited torsional response to the ground excitation. The seismic performance of the building is simulated in this study with a three-dimensional model of the building which utilizes the strut modeling approach for infilled frames. The struts are calibrated using a novel approach which is based on a recently proposed simplified analytical tool for such structures. The simplified tool is validated with detailed FE models that combine the smeared and the discrete crack modeling approaches. The paper discusses the accuracy of the numerical model in simulating the seismic performance and in estimating the identified modal properties of the damaged building. The comparison indicates that the model, when subjected to the ground motion recorded in close proximity during the Gorkha earthquake, develops a similar damage pattern as the actual structure, while its modal properties match well with those estimated from the ambient vibration recordings obtained during a reconnaissance trip.

Keywords: Masonry infill, RC frame, 2015 Nepal Earthquake, nonlinear modeling, finite element modeling, strut modeling

1. Introduction

On April 25, 2015, a devastating, 7.8 M_w, shallow earthquake, with a focal depth of 8.2 km [1] struck Nepal. The epicenter was located in Lamjung, Gorkha district, 75 km northeast of Kathmandu. This earthquake was followed by 400 aftershocks of magnitudes larger than 4.0 M_w, including three of magnitudes of 6.6, 6.7 and 7.3 M_w with epicenters in the districts of Gorkha and Dolakha. The seismic sequence caused more than 9,000 fatalities, almost 25,000 injuries and damaged beyond repair over 500,000 buildings [2].

The earthquake was rather destructive in the Kathmandu Valley which is 100 km from the epicenter. This is due to the characteristics of the unconsolidated and slightly consolidated soils of the Kathmandu region (Fig.1a). The soft soil deposits filtered the seismic motion of the rock outcrop which was similar to the recording at the KTP station. This station is located at a firm rock site and recorded maximum peak ground acceleration (PGA) of 0.260g and does not include the long period pulses observed in the horizontal accelerograms recorded at the sedimentary sites (KATNP, TVU, PTN and THM stations) which are affected by the response of the soil deposits. All available ground motions due to the main shock recorded in the Kathmandu area by USGS and the stations of Institute of Seismology and Volcanology, at Hokkaido University, Japan [3] are shown in Fig. 1b.

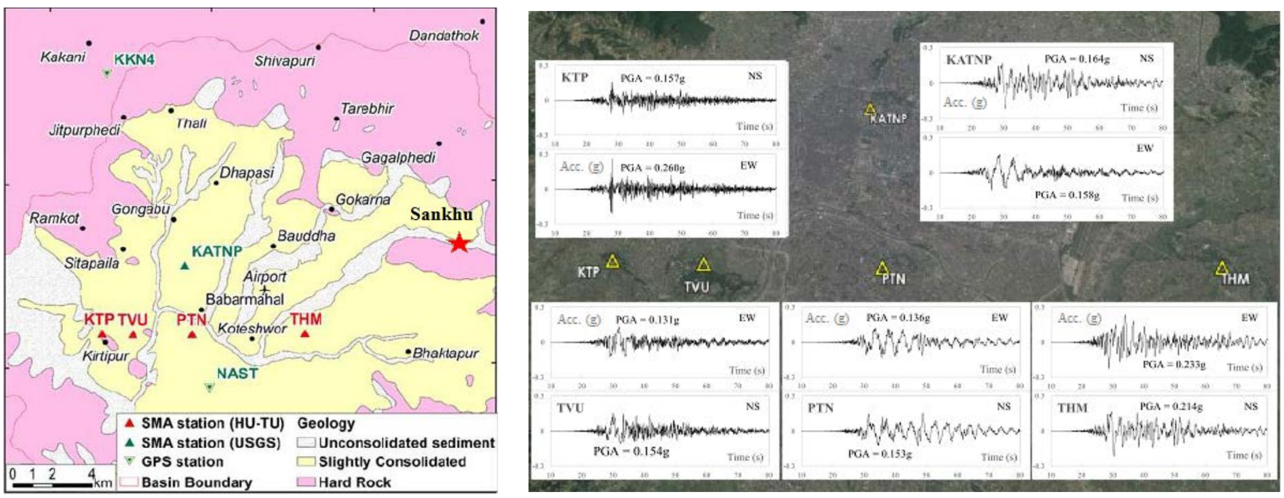

(a) soil conditions (b) acceleration time histories

Fig. 1 – (a) Local soil conditions around Kathmandu and (b) acceleration time histories of mainshock [3-5]

This paper focuses on a four-story school building in Sankhu, a town located 13 km north-east of Kathmandu and 87 km from the epicenter. The building had a masonry-infilled reinforced concrete (RC) frame. It was severely damaged during the 2015 Gorkha earthquake and was red-tagged by the local engineers. The damage was mostly concentrated towards the south end of the ground story, probably due to torsional response to the ground excitation, primarily induced by the increased stiffness provided by the stair cases in the north end. The dimensions of the structure along with the design details and material properties were obtained by in situ measurements during a reconnaissance study [1], two months after the earthquake. During this visit, the structure was also instrumented with four unidirectional accelerometers at each story level to collect ambient vibration data. The modal parameters of the building such as the natural frequencies, mode shapes, and damping ratios are identified using the Natural Excitation Technique combined with the Eigen-system Realization Algorithm (NExT-ERA), an operational modal analysis method. A finite element (FE) model of the damaged school building is developed using struts, to simulate the effect of the masonry infills, in order to model the building's behavior during the ground motion. The model is based on a recently proposed methodology [6,7] and is validated by comparing the obtained force displacement plots to those estimated using a detailed finite element model employed to simulate the performance of each individual bay of the ground floor. The model is also validated with the identified modal parameters obtained from the recorded ambient vibration data. The validated numerical model is used to simulate the response of the structure during the Gorkha earthquake and provides insight into the observed failure mechanism of the school building.

2. Structural Details, Seismic Damage and Instrumentation Layout

2.1. Four-Story infilled RC school building

The four-story school building located in Sankhu, Nepal (27.7273N, 85.4619E) is shown in Fig. 2. The building has relatively simple structural system consisting of an RC frame of seven bays on the north-south direction and two bays in the east-west direction. The bays in the west side of the building are not infilled as they form a corridor, which is exposed to the weather. On the contrary, the bays in the east side, along line 1 of Fig.2b are infilled and have a wide but relatively short window, while in the bays along line 2 of Fig. 2b have larger windows and/or doors. The stair cases are located towards the north end, thus inducing horizontal irregularity in the structure.

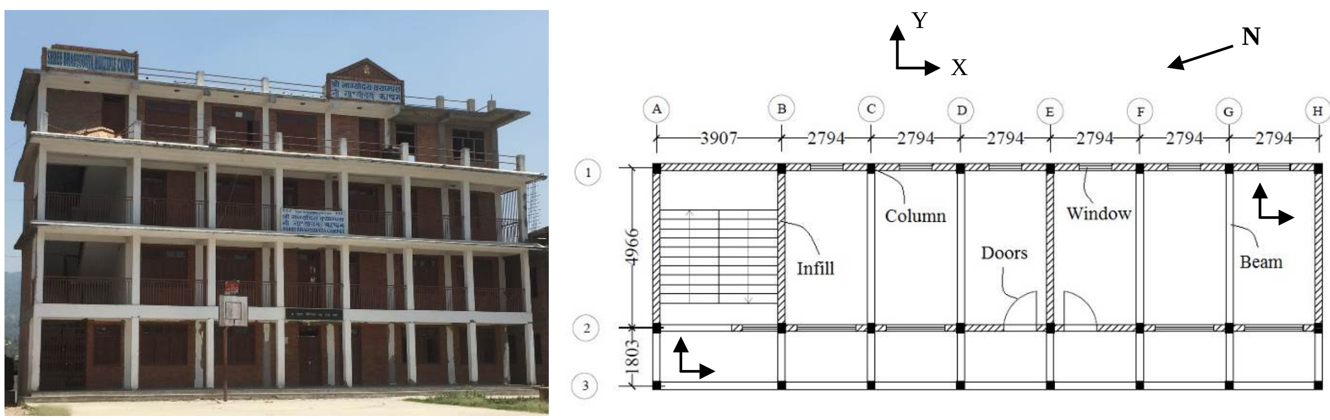

(a) west elevation view (b) plan view (dimensions in mm)

Fig. 2 – Four-story school building at Sankhu

2.2. Observed Damage

After the seismic sequence, shear failure in the columns and extensive damage in the beam-column joints in the south end of the ground story was observed, as shown in Fig. 3a to 3d. This distribution of damage can be probably attributed to the staircases which shifted the center of rigidity towards the North end introducing torsion to the structure. The damaged columns also revealed inadequate reinforcement detailing and spacing of stirrups, in addition to poor construction. Examples of damage in the infill panels that were separated from the bounding frame, including dominant diagonal and horizontal cracks, are shown in Fig. 3e and 3f.

2.3. Instrumentation Layout for Ambient Vibration Recordings

The ambient vibration was recorded using 12 accelerometers in two setups. In the first setup, A, the accelerometers were installed on the roof, and the 4th- and 3rd-story slabs. For the second setup, B, the instruments from the top two slabs were moved to the 2nd story and the ground floor. Those accelerometers on the 3rd floor were kept in the same locations as Setup A, to provide reference measurements between the two setups. In each floor level, four accelerometers were installed at two opposite corners of the building, namely the North-West and the South-East corners as shown in Fig. 2b, to measure the acceleration response at two perpendicular directions, named as X and Y directions. A total of 54 and 45 minutes of ambient vibrations were recorded for Setups A and B, respectively.

(a) Column G1 (b) Column G2 (c) Column H1 (d) Column H2

(e) infill panel H12 (f) infill panel E12

Fig. 3 – Damages observed in the first-story of the school building at Sankhu during the earthquake

3. Finite Element Models

A three-dimensional finite element model of the four-story school building in Sankhu is developed in the structural analysis software OpenSEES [8] using the strut approach. The model utilizes beam-column elements discretized in fibers for the RC beams and columns. Diagonal truss elements are used to simulate the effect of the infill walls on the lateral response. The geometry of the model is based on the analysis of point cloud data obtained with LiDAR cameras, complimented with *in situ* measurements. The material properties used in the model, summarized in Table 1, are based on the material tests reported in [9,10] . The elastic modulus and yield strength of rebars are assumed to be 2×10^5 MPa (29000 ksi) and 414 MPa (60 ksi), respectively.

Table 1 – Material properties of concrete and masonry

Parameters	**Elastic Modulus MPa (ksi)**	**Compressive Strength MPa (ksi)**	**Tensile Strength MPa (ksi)**	**Coefficient of friction**	**Cohesion MPa(ksi)**
Concrete	13941 (2022)	9.71 (1.40)	1.38 (0.20)	-	-
Masonry	2551 (370)	3.44 (0.50)	1.03 (0.15)	0.90	0.34 (0.05)

To calibrate the struts, the framework proposed by Stavridis [11] is applied. Based on this modeling methodology, the backbone curve for each infilled bay of the structure is derived first using simple equations. The methodology is modified here, by reducing the estimated initial stiffness by 40% to account for the potential cracks and damage of the structure prior to the earthquake [12].

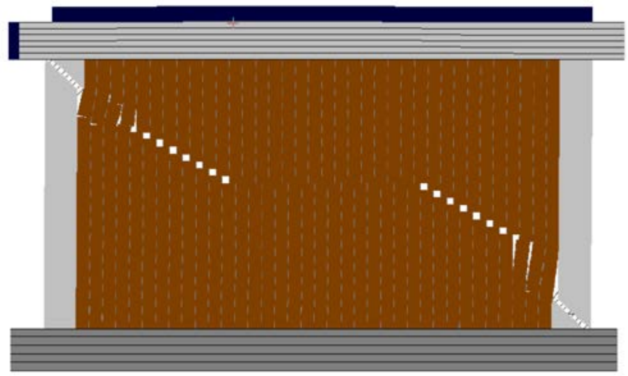

Fig. 4 – Deformed shape of FE model of Panel E.

To facilitate the application of the modeling framework, the infilled bays of the building are grouped in seven types based on the dimensions, opening geometry and tributary area affecting the gravity loads (Fig. 7a). Finite element models of these single-story single-bay frames are also developed in FEAP [13] following a modeling methodology that combines the smeared-crack and interface elements [14] which allows the simulation of dominant shear and diffused flexural cracks in the RC members, the crushing and tensile splitting of the masonry units, and the mixed-mode failure of the mortar joints. As it can be seen in Fig. 4, the failure pattern of the model of Panel E subjected to monotonic pushover analysis is similar to the actual damage pattern induced in that panel during the earthquake as shown in Fig. 3f.

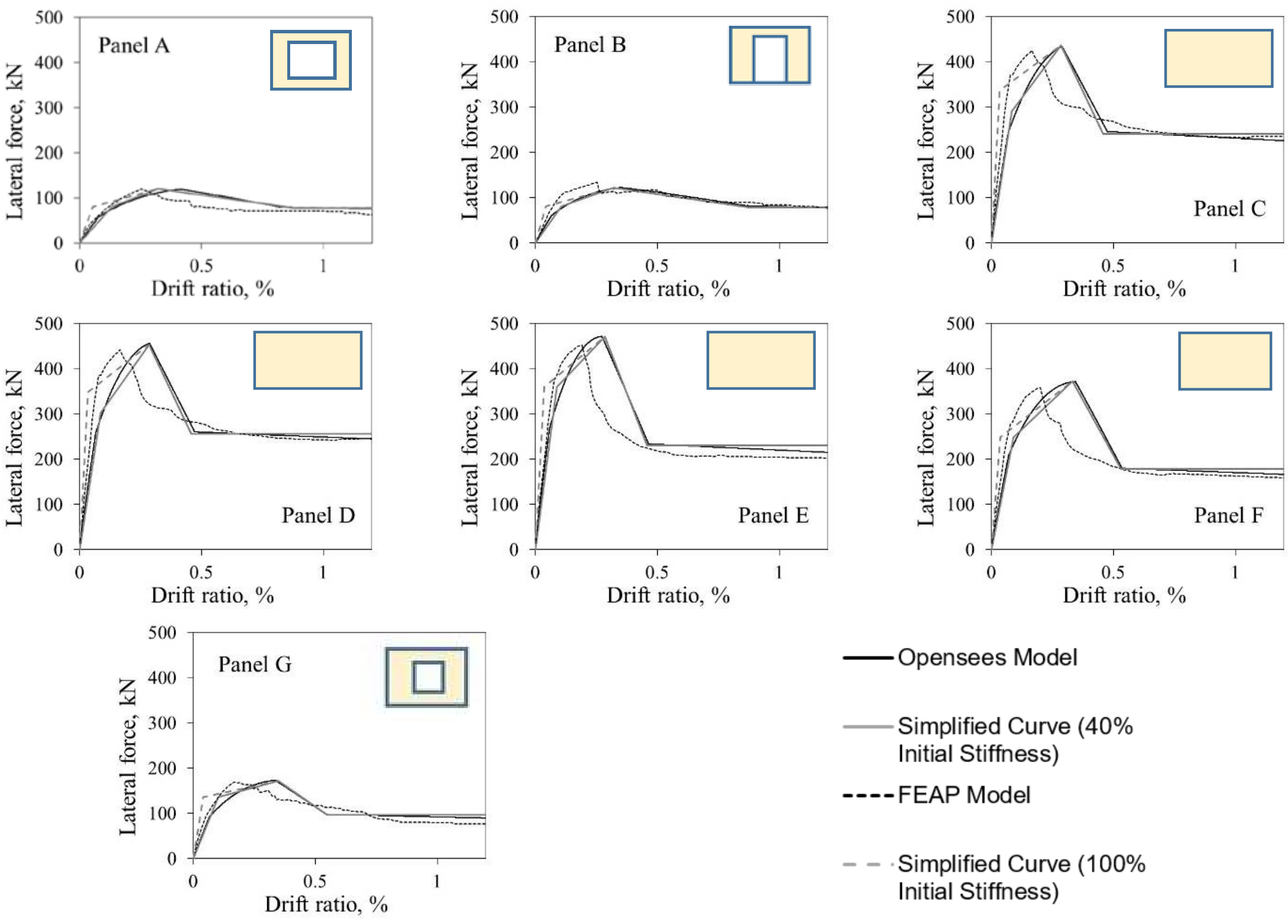

Fig. 5 – Calibrated response of single-story single-bay frame.

The comparison of the force-vs.-displacement curves (Fig. 5) obtained analytically and numerically indicates that the analytically developed curves capture accurately the strength of the infilled frames but tend to underestimate the stiffness and overestimate the drift at peak strength. This is more pronounced for the cases of Panels A and B that include large openings. The discrepancy can be expected as the study based on which the simplified curves are developed [11], considered solid panels and panels with openings smaller than 25% of the panel total area. Therefore, for infill panels A and B, that include large openings with areas larger than 40% of the bay area, the simplified curves have been modified to better match the detailed FE analysis.

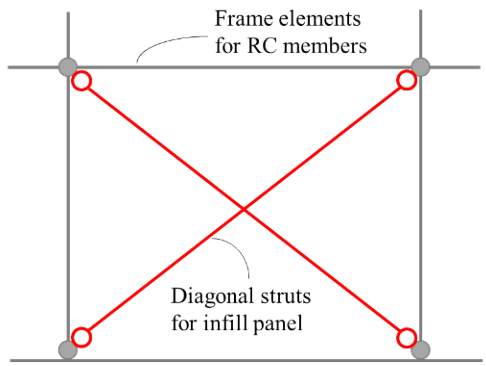

(a) single-bay, single-story infilled frame

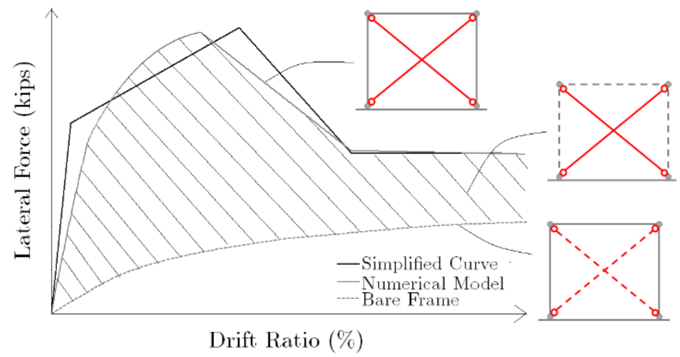

(b) simplified analytical tool

Fig. 6 – Simplified analytical tool for development of strut model

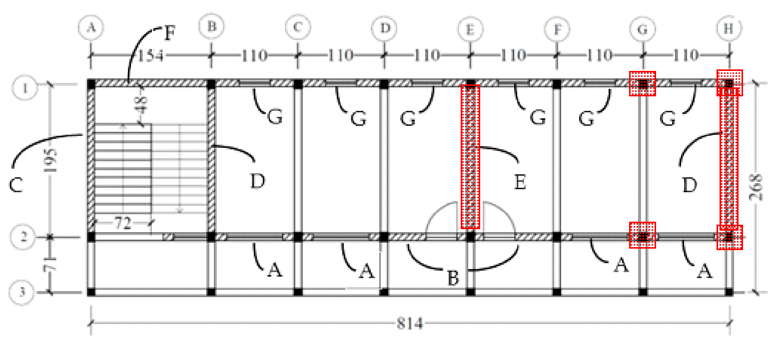

(a) different types of infill panel

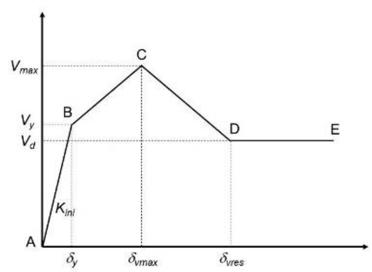

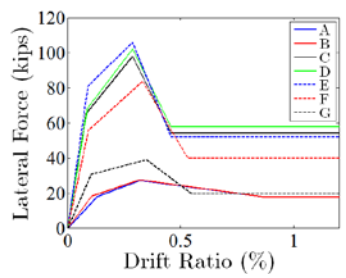

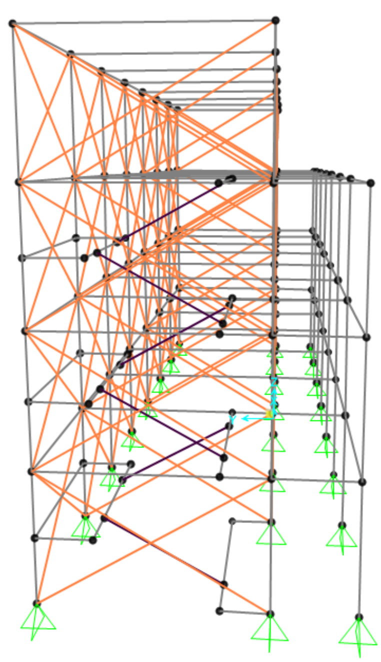

(b) force vs. displacement curves (c) estimation of simplified curve (d) diagonal strut model

Fig. 7 – Simplified curves for single-story single-bay frames and 3D diagonal strut model

Once the backbone force-vs.-displacement curves are developed, they are used to calibrate the struts representing the masonry infills. This is achieved using a distinct single-bay, single-story numerical model for every bay of the building in OpenSEES (Fig. 6a). The Menegotto-Pinto [15] steel model is used for the steel rebars, while for the concrete and masonry, the Concrete02 material model from the Opensees material library is used [16]. The concrete and the steel models are calibrated with the material properties summarized in Table 1. The diagonal struts are calibrated so that when added to the model of the single-bay RC frame, the resulting lateral force-vs.-displacement curve is similar to the curve derived analytically for that frame (Fig. 6b). The thickness of the diagonal struts is kept equal to the infill thickness in the building, i.e., 23 cm (9 in). The strut width, the strains at peak strength, and the strains at the onset of the residual strength are selected so that the calibrated lateral force-vs.-drift response of the corresponding infilled frames match the simplified curves as shown in Fig. 5. Once the diagonal struts are calibrated, the thee-dimensional model of an entire building, consisting of 428 frame elements shown in Fig. 7d is assembled in OpenSEES.

3.1 Estimation of earthquake response

The three-dimensional numerical model of the structure was subjected to the two components of the ground motion recorded at the THM (27.6818N, 85.2883E) station which was closest to the building as indicated in Fig. 1.The results of the nonlinear time-history analysis indicate that the structure demonstrated significant torsional response. This can be observed in the peak and residual inter-story drifts measured at the four corners of the structure which are summarized in Table 2. The deformations at the bottom story are in all cases significantly higher than those in the upper stories. Moreover, in the two columns in the south side of the building, along line H, the drifts in the Y direction are the largest observed with the peak first-story drift being 1.83% compared to 0.28% for the north columns. The residual drifts are also considerably larger exceeding 0.2%, while in the north side the residual drifts are 40% of that value. The larger deformations in the south end indicate the torsional response of the building during the seismic excitation. Moreover, the peak and residual drifts in the upper stories are relatively small indicating the formation of a soft-story mechanism as the damage is concentrated in the first story of the model. The peak strains in the longitudinal bars of the first-story columns towards the south end considerably exceeded the assumed yield strain of 0.0021, however those towards the north end are considerably smaller. The estimated strain values on the beam reinforcement are lower than 200 $\mu\varepsilon$ indicating that the beams did not develop significant damage as observed in the structure.

Table 2 –Inter-story drift in the four corners of the structure predicted by the numerical model.

Quantity	**Location**		**Peak**		**Residual**	
			X	**Y**	**X**	**Y**
Inter-Story Drift (%)	A1	Story-1	0.16	0.28	0.01	0.05
		Story-2	0.07	0.04	0.002	0.001
		Story-3	0.03	0.06	0.001	0
		Story-4	0.03	0.04	0	0.001
	A3	Story-1	0.30	0.28	0.08	0.05
		Story-2	0.13	0.04	0.002	0.001
		Story-3	0.08	0.06	0.003	0.001
		Story-4	0.04	0.04	0	0
	H1	Story-1	0.16	1.83	0.01	0.21
		Story-2	0.07	0.21	0.002	0.002
		Story-3	0.03	0.17	0.001	0.003
		Story-4	0.03	0.19	0	0.001
	H3	Story-1	0.30	1.83	0.08	0.21
		Story-2	0.13	0.21	0.002	0.003
		Story-3	0.09	0.17	0.003	0.002
		Story-4	0.04	0.19	0	0.002
Axial Strain ($\mu\varepsilon$)	Column-A1		1261		108	
	Column-A3		1741		138	
	Column-H1		3204		2211	
	Column-H3		2989		2225	
	Beam-H12		193		78	
	Beam-1AB		187		31	

The lateral force-vs.-drift response of the east-west infill panels and the bounding RC columns along the lines A, B, E and H of the first story are presented in Fig.8 to Fig. 10. The figures indicate the torsional response of the structure and the different force demands on the columns and the infills. This is evident as despite the similar stiffness and strength (460kN), the panels towards the south (H12 and E12) reached story drift close to 1%, much higher than those for the panels towards the north (A12 and B12). All the RC columns remained within the linear range along X-direction with the maximum strength less than 15kN and maximum drift close to 0.25%. On the contrary, the RC columns along the lines E and H towards the south end exhibited nonlinear behavior in Y direction, with the maximum drift reaching values close to 2%, while the columns towards the north end remain within the linear zone. The non-linear behavior and considerable deformation of the members (Table 2) towards the south end of the building along the Y direction match well with the observed damage pattern.

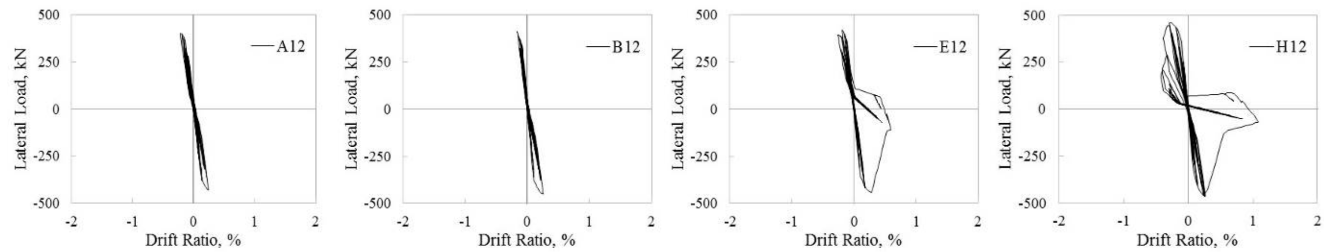

Fig. 8 – Lateral force-vs.-story drift along Y direction of the first story infill panels A12, B12, E12 and H12

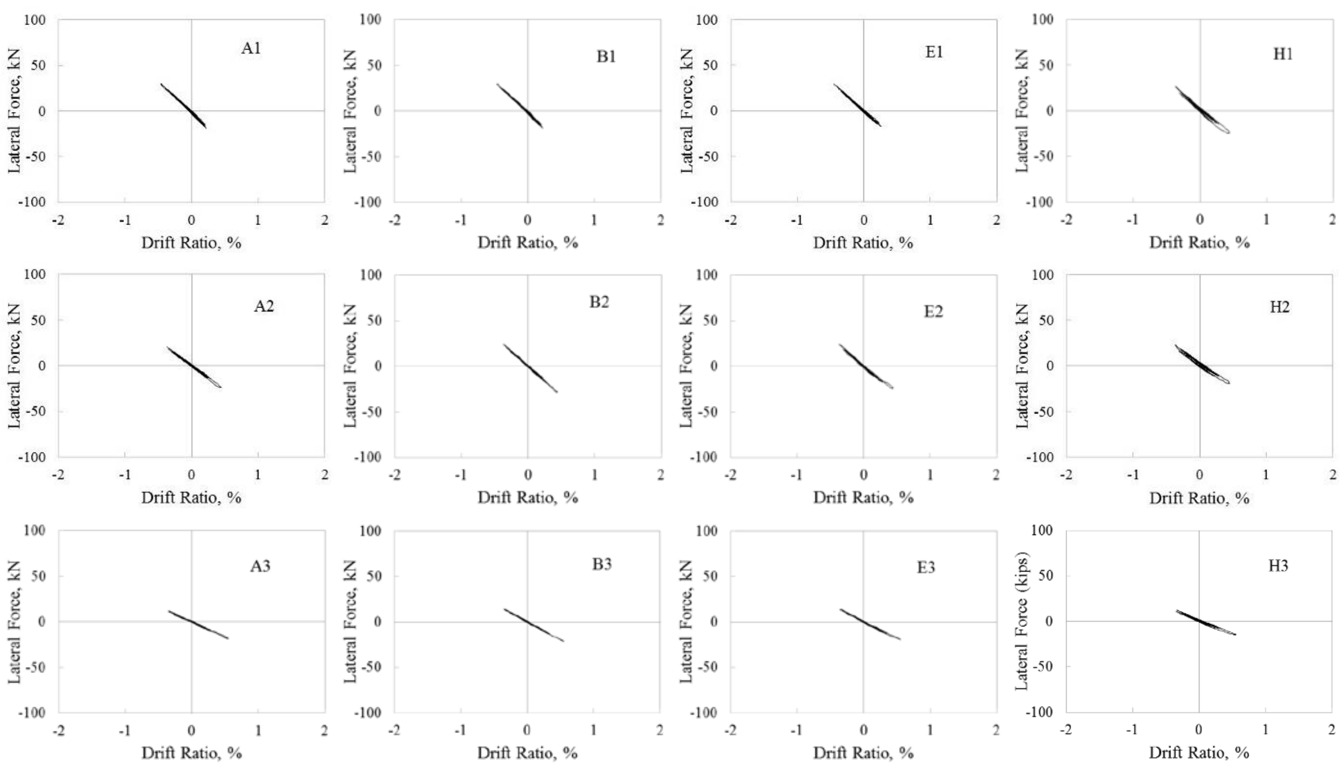

Fig. 9 – Lateral force-vs.-drift along X direction of the first story columns

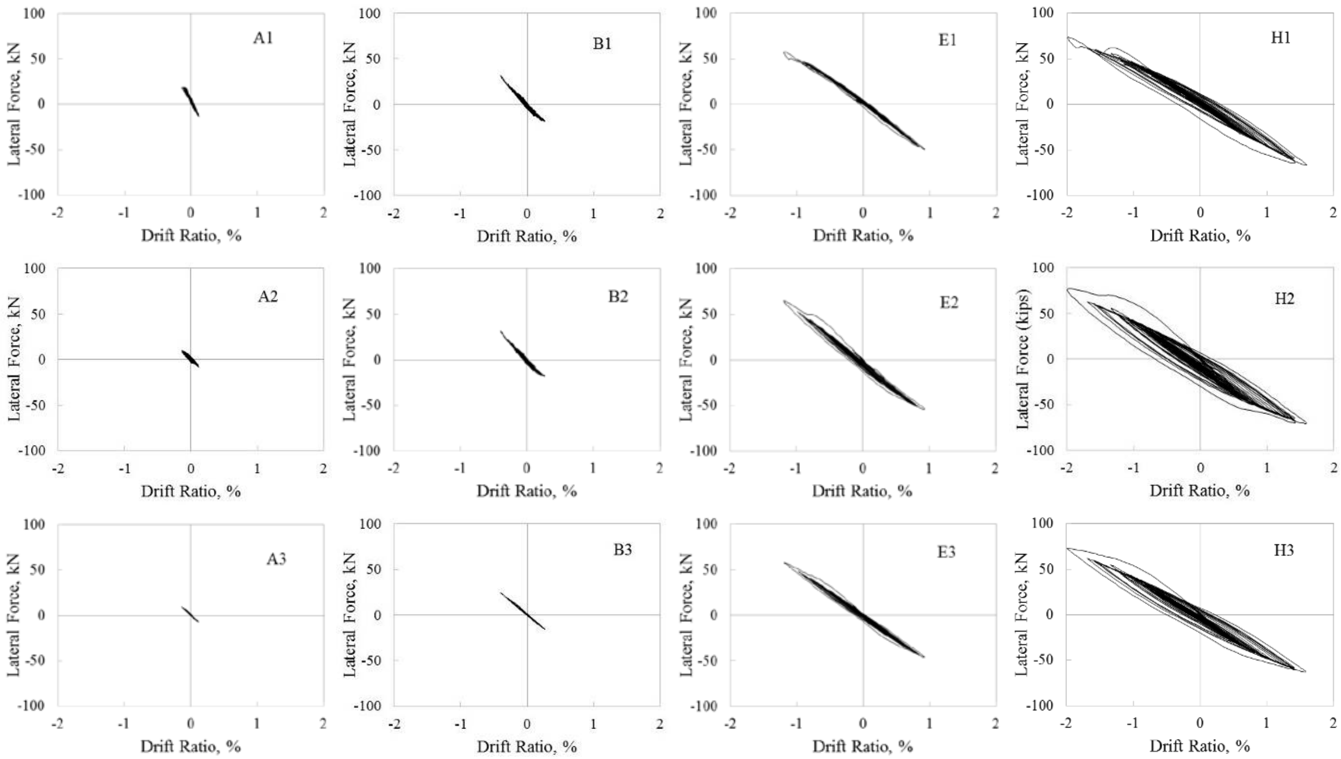

Fig. 10 – Lateral force-vs.-drift along Y direction of the first story columns

4. System Identification

In the application of system identification, eleven 9-minute long data sets are considered, resulting in six sets of modal parameters for Setup A and five for Setup B. The data are filtered using a band-pass (1.0-8.0 Hz) Finite Impulse Response (FIR) filter of order 4096. The filtered response is then down-sampled from 2048 to 256 Hz to increase the computational efficiency. The Natural Excitation Technique combined with the Eigensystem Realization Algorithm (NExT-ERA) is employed to identify the natural frequencies of the structure. The NExT-ERA method is an output-only parametric system identification approach which estimates the modal parameters of a linear dynamic system from its measured response to a broadband excitation [17-19]. Two reference channels are used in the system identification to account for excitations in both directions. More information on the system identification study can be found in [19, 20].

5. Model Validation

The identified natural frequencies and mode shapes estimated from the ambient vibration recordings are used to validate the numerical model. This can be achieved by comparing the identified modal properties with the corresponding modal properties of the model after it is subjected to the ground motion recorded at THM station. The modal frequencies obtained from the numerical model are compared to those identified from the ambient vibration recordings in Table 3. It can be observed that the natural frequencies of the structure obtained from the finite element model for the first three modes are close to those estimated from the ambient vibration data. The frequencies estimated from the finite element model are all higher than the identified frequencies. This is because the aftershocks, which may have induced additional damage to the building have not been considered in this study since the ground motion records are not available. The mode shapes obtained from the numerical model are compared with the identified mode shapes in Fig.11 and the Modal Assurance Criterion (MAC) values, which are summarized in Table 3. The MAC values are in all cases higher than 90%. Given the simplicity of the model this is a very good agreement considering the complexity involved with modelling the seismic response of an actual structure to bi-directional ground shaking.

A simpler but as accurate approach way to evaluate the accuracy of the model, is to remove the elements representing the severely damaged columns and infills in the ground floor and compare the modal properties of that model with the identified ones. The removed elements are shown in Fig.6 and include the RC columns: H1, H2, G1, G2 and Infill Panels: H12 and E12 of the first story. In this case, the estimated frequencies are even higher, indicating that other members of the structure have been damaged besides the ones removed. However, the match between identified and estimated frequencies is very good considering the simplified modeling approach.

Table 3 – Comparison of frequencies obtained from ambient vibration data and finite element model

Mode	Original Frequency (Hz)	Natural Frequency (Hz) after mainshock					
		Ambient Vibration	Finite Element		Error (%)		
			Non-Linear	Linear	Non-Linear	Linear	
1	2.61	1.19	1.32	1.30	11.39	9.45	
2	2.83	2.15	2.31	2.69	7.44	25.03	
3	3.69	3.17	3.23	3.39	1.89	6.93	

Table 4 – MAC values of identified mode shapes compared with numerical model mode shapes

Mode	1	2	3
Linear	0.99	0.95	0.95
Non-Linear	0.99	0.95	0.92

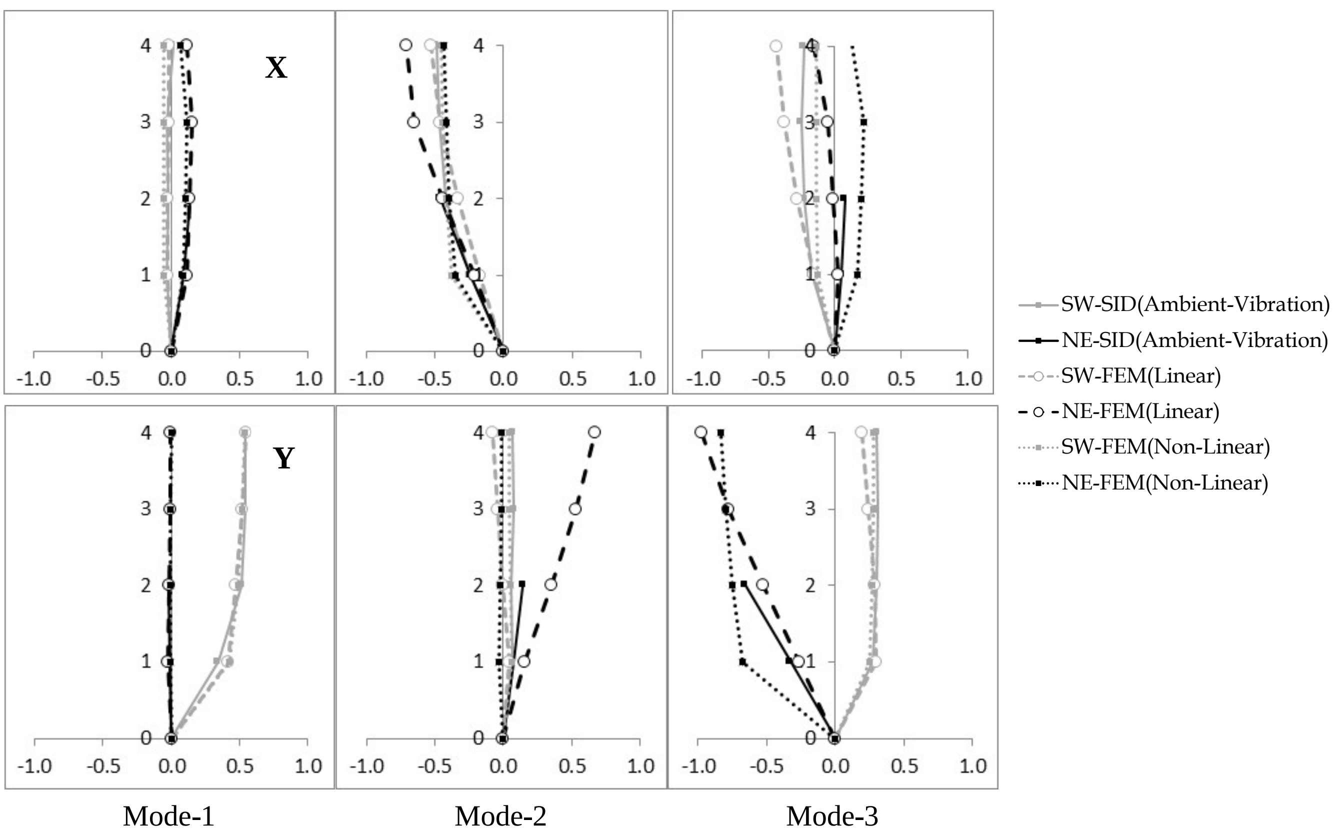

Fig. 11 – Comparisons of mode shapes obtained from numerical model and ambient vibration recordings

6. Conclusions

This paper presents the nonlinear modeling of the bi-directional seismic response of a four-story masonry-infilled reinforced concrete frame building in Sankhu, Nepal, which was severely damaged during the 2015 Gorkha earthquake. The damage in the school building was concentrated towards the south end in the first story indicating that the structure exhibited torsional response to the ground excitation. A simplified finite element model of the structure is developed using a simple method to estimate the force-displacement curve of each individual bay. The strut elements are employed to simulate the structural performance of the infilled walls following a novel calibration approach. The comparison of the predicted and the actual damage patterns indicates that the model can accurately simulate the torsional response of the actual structure. Moreover, the obtained modal parameters after subjecting the numerical model to the horizontal ground motions are compared to the modal parameters identified from the ambient vibration recordings. The natural frequencies and mode shapes of the first three modes estimated from the system identification are in good agreement with those from the finite element model. Moreover, the identified modal frequencies and mode shapes are compared with those obtained from the model after the six severely damaged members are removed. The predicted frequencies, although higher, are close to the identified ones in this case as well, indicating that there is additional damage in the structure.

7. Acknowledgements

Partial support of this study by the National Science Foundation Grants 1254338 and 1545595 is gratefully acknowledged. The authors would also like to acknowledge the support of National Society of Earthquake Technology (NSET) in Nepal, through the support of Ramesh Guragain and Dev Kumar Maharjan. The collaboration of other researchers including Andre Barbosa, Richard Wood, Dan Gillins, Patrick Burns, Matt Gillins, Michael Olsen, Giuseppe Brando, Davide Rapone, Enrico Spacone, Rajendra Soti, Humberto Varum, António Arêde, Nelson Vila-Pouca, André Furtado, João Oliveira, Hugo Rodrigues, Marco Faggella and Rosario Gigliotti during the reconnaissance trip and in the collection of data is greatly appreciated as well. However, the opinions expressed in this paper are those of the authors and do not necessarily represent those of the sponsor or the collaborators.

8. References

[1] Brando G, Rapone D, Spacone E, Barbosa A, Olsen M, Gillins D, Soti R, Varum H, Arede A, Vila-Pouca N, Furtado A, Oliveira J, Rodriges H, Stavridis A, Bose S, Faggella M, Gigliotti R, Wood RL (2015): Reconnaissance report on the 2015 Gorkha earthquake effects in Nepal. *XVI ANIDIS*, L'AQUILA, Italy.

[2] Rai DC, Singhal V, Raj BS, Sagar L (2015): Reconnaissance of the effects of the M7.8 Gorkha (Nepal) earthquake of April 25, 2015. *Journal of Geomatics, Natural Hazards and Risk, Taylor and Francis*, **7** (1), 1-17.

[3] Takai N, Shigefuji M, Rajaure S, Bijukchhen S, Ichiyanagi M, Dhital M R, Sasatani T (2016): Strong Ground Motion in the Kathmandu Valley during the 2015 Gorkha, Nepal, Earthquake. *Earth Planets and Space*, **68** (10)

[4] United State Geological Survey (2015): http://earthquake.usgs.gov/earthquakes/eventpage/us20002926#scientific_waveforms USGS.

[5] Moss RES, Thompson EM, Kieffer DS, Tiwari B, Hashash YMA, Acharya I, Adhikari B, Asimaki D, Clahan KB, Collins BD, Dahal S, Jibson RW, Khadka D, Macdonald A, Madugo CLM, Mason HB, Pehlivan M, Rayamajhi D, Uprety S (2015): Geotechnical Effects of the 2015 Magnitude 7.8 Gorkha, Nepal, Earthquake and Aftershocks. *Seismological Research Letters*.

[6] Reese A, and Stavridis A (2014): A simplified method for the estimation of the seismic resistance of RC frames with weak infill panels. *In NCEE 2014 - 10th U.S. National Conference on Earthquake Engineering: Frontiers of Earthquake Engineering*. Earthquake Engineering Research Institute.

[7] Martin Tempestti, A. Stavridis. "Simplified method to assess lateral resistance of infilled reinforced concrete frames." *Proc. 16th World Conference in Earthquake Engineering*, Santiago Chile, January 2017.

[8] McKenna F, Fenves GL, Scott MH, Jeremic B (2000): *Open system for earthquake engineering Simulation* (*Opensees*), Pacific Earthquake Engineering Research Center, University of California, Berkeley, CA.

[9] Chaulagain H, Rodrigues H, Spacone E, Varum H, (2014): Seismic assessment of RC structures with infill masonry panels in Nepal - Sensitivity analysis. *Second European Conference on Earthquake Engineering and Seismology*, Istanbul, Turkey

[10] Pradhan PL (2009): Composite actions of brick infill wall in RC frame under in-plane lateral load. *PhD Dissertation*, Tribhuvan University, Pulchowk Campus.

[11] Stavridis A (2009): Analytical and experimental study of seismic performance of reinforced concrete frames infilled with masonry walls. *PhD Dissertation*, University of California, San Diego.

[12] ACI 369 (2011): Guide for Seismic Rehabilitation of Existing Concrete Frame Buildings and Commentary, *American Concrete Institute*

[13] Taylor RL (2007): *FEAP - A Finite Element Analysis Program - Version 8.1*. Manual. Dept. of Civil and Environmental Engineering, University of California at Berkeley, Berkeley, California.

[14] Stavridis A, Shing PB (2010): Finite element modeling of nonlinear behavior of masonry-infilled RC frames. Journal of Structural Engineering, **136**(3):285–96.

[15] Menegotto M, Pinto, PE (1973): Method of analysis for cyclically loaded reinforced concrete plane frames including changes in geometry and non-elastic behavior of elements under combined normal force and bending. *IASBE Symposium on Resistance and Ultimate Deformability of structures Acted on by Well-Defined Repeated Loads*, Final Report, Lisbon.

[16] Hisham M, Yassin M (1994): Nonlinear Analysis of Pre-stressed Concrete Structures under Monotonic and Cycling Loads, *PhD dissertation*, University of California, Berkeley.

[17] Junag JN, Pappa RS (1985): An eigensystem realization algorithm for modal parameter identification and model reduction. *Journal of guidance, control, and dynamics*, **8**(5), 620-627.

[18] Farrar C, James III G (1997): System identification from ambient vibration measurements on a bridge. *Journal of Sound and Vibration*, **205**(1), 1-18.

[19] Moaveni B, Barbosa AR, Conte JP, Hemez FM (2014): Uncertainty analysis of system identification results obtained for a seven story building slice tested on the UCSD-NEES shake table. *Structural Control and Health Monitoring*, **21**(4), 466-483.

[20] Bose S, Nozari A, Mohammadi ME, Stavridis A, Moaveni B, Wood R, Gillins D, Barbosa A (2016): Structural Assessment of a school building in Sankhu, Nepal damaged due to torsional response during the 2015 Gorkha earthquake. Proceedings of International Modal Analysis Conference, 34th IMAC, Orlando, Florida.